Journal of Materials Science and Chemical Engineering, 2025, 13(9), 155-164
https://www.scirp.org/journal/msce
ISSN Online: 2327-6053
ISSN Print: 2327-6045

Research on High-Resolution Imaging Method of Precious Metal Particles Based on Contrast Difference

Li Liu[1,2], Ning Liu[1,2], Zengbin Wang[1,2], Zhengang Zhang[1,2], Liqiang Dai[1,2], Kaixuan Lang[1,2]

[1]Weichai Power Co., Ltd., Weifang, China
[2]National Internal Combustion Engine Industry Measurement and Testing Center, Weifang, China
Email: llichess@126.com

How to cite this paper: Liu, L., Liu, N., Wang, Z.B., Zhang, Z.G., Dai, L.Q. and Lang, K.X. (2025) Research on High-Resolution Imaging Method of Precious Metal Particles Based on Contrast Difference. *Journal of Materials Science and Chemical Engineering*, **13**, 155-164.
https://doi.org/10.4236/msce.2025.139010

Received: August 13, 2025
Accepted: September 20, 2025
Published: September 23, 2025

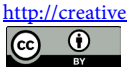

Abstract

As one of the important research methods for nanomaterial analysis, transmission electron microscopy (TEM) uses high-energy electron penetration of the sample to achieve high-resolution imaging and intuitively analyze surface morphology, atomic-level lattice structure, element distribution, and other information. At present, supported precious metals, such as Pt and Pd, are widely used in the field of industrial catalysis, and in the atomic-scale characterization of supported precious metal catalysts, the difference in contrast resolution with different imaging contrasts makes it difficult to effectively distinguish between precious metal particles and catalyst supports. Based on this challenge, this paper systematically expounds the imaging principle, detection method system, and test optimization of transmission electron microscopy, providing ideas and theoretical support for solving the atomic-scale detection of supported precious metal catalysts. Taking platinum/carbon catalysts and diesel engine oxidation catalysts as examples, the results show that platinum-carbon catalysts are more suitable for bright-field imaging due to the large atomic number (Z) difference between carbon support and platinum particles and the influence of electron beam sensitivity, while diesel engine oxidation catalysts with moderate polymetallic Z difference and stable support are more suitable for high-angle annular dark-field images (HAADF). At the same time, the combined technology of X-ray spectroscopy and transmission electron microscopy has unique advantages in the elemental composition analysis of supported precious metal catalysts.

Keywords

Transmission Electron Microscope, Loaded Catalyst, Precious Metal Nanoparticles, High-Resolution Imaging

1. Introduction

Energy is an important pillar of modern social development, and the pressure on energy supply is increasing in the context of global economic transformation and lifestyle transformation [1]-[3]. As a key technology for realizing the green chemistry and energy revolution, catalysis plays an important strategic role in clean energy conversion and efficient energy utilization. From the perspective of the evolution of catalytic systems, although homogeneous catalysts have ideal reactivity and product selectivity, there are problems such as metal residue pollution, and non-homogeneous catalytic systems make up for this defect and gradually become an irreplaceable advantage in the field of modern catalysis. As a core component of heterogeneous catalyst systems, supported precious metal catalysts occupy a key position in modern industrial catalysis, such as automobile exhaust purification and fuel cells, due to their excellent catalytic activity and controllability. With the development of nanotechnology, material surface science, and other disciplines, the development and application of new supported precious metal catalytic systems, such as single-atom catalysts and alloy catalysts, have been deepened and have become the key research direction in the current field of catalysis. In the study of catalytic reaction mechanisms, researchers optimize the design and support properties of precious metals by regulating the size, morphology, component optimization, and support performance. Therefore, how to capture the key information of catalysis at the nanometer or even atomic resolution is particularly important for the fine design of catalyst performance.

Transmission electron microscopy is one of the important means for the characterization of catalytic materials, which can provide a new dimension of microscopic observation for the study of energy catalytic materials through multimodal imaging capabilities [4] [5]. At present, transmission electron microscopy has transmission mode, diffraction mode, and scanning transmission, among which bright-field imaging (BF-TEM) can observe metal dispersion and support uniformity, and high-angle annular dark-field imaging (HADDF-STEM) can accurately identify single-atom catalytic sites. In addition, the imaging mode is combined with spectroscopic techniques such as X-ray energy dispersive spectroscopy (EDS) to obtain nanostructure morphology information, as well as in-depth analysis of the electron element distribution. It is worth noting that the contrast differences generated by different modes are easy to ignore during TEM observation, and it is impossible to quickly distinguish between precious metal particles and catalyst supports.

2. Function Description and Principle

2.1. Equipment Description

Transmission electron microscope is an electron optical equipment that uses electron lenses with extremely short wavelengths as the illumination source and uses electromagnetic lenses to achieve high-magnification focused imaging, and its architecture is based on the coordinated operation of electron optical system, vac-

uum system and electrical system, of which the electron optical system is mainly composed of illumination system, objective/goniometer and imaging system, which is an important part of transmission electron microscope [6] [7]. The illumination system is composed of an electron gun, a condenser and a tilt adjustment device, the electron gun is an emission source made of tungsten wire or lanthanum hexaboride, and the emitted electrons are irradiated to the sample in the form of a divergent beam or a focusing beam, and the electron beam aperture angle is reduced through the small aperture condenser diaphragm to form a parallel beam. The core part of the objective lens, sample rod, and goniometer system is usually located in the central area of the transmission electron microscope, where the diffraction pattern and sample image can be seen on the back focal plane and image plane. The imaging system collects electrons from the sample emission surface by the objective lens, and the scattered electrons form a diffraction pattern on the back focal plane and then recombine them in the image plane for imaging [8]-[10]. Vacuum systems include mechanical pumps, diffusion pumps, cryogenic pumps, etc. Maintaining a good vacuum environment is extremely important for sample observation.

2.2. Imaging Principle

2.2.1. Bright-Field Image

A bright-field image is the most basic imaging mode. When observing the sample, SADP projection is performed on the fluorescent screen/CCD for imaging operation, the selected diaphragm is moved out in the image mode, the objective lens focuses the image, and the direct transmission beam electronic signal is collected to obtain the bright-field image. The bright-field image includes two mechanisms: mass-thickness contrast and diffraction contrast, the mass thickness contrast is related to the atomic number of the sample, the local thickness, the contrast is generally the difference in the scattering ability of the electron beam in different regions, the high scattering region appears as dark color in the image, and the low scattering area appears as bright color in the image. The schematic diagram of the quality-thickness contrast under the bright-field image is shown in **Figure 1**.

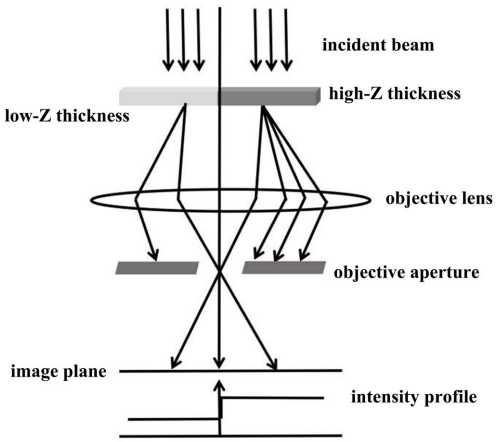

Figure 1. Schematic diagram of quality-thickness contrast (bright-field image).

2.2.2. High Angle Circular Dark Field Image

The annular dark-field image is realized by a ring detector surrounding the BF detector, and the high-angle annular dark-field image is formed by receiving high-angle scattered electrons to participate in the imaging. Z-contrast is an atomic-level high-resolution imaging technology, which has the advantage of being stable and unaffected even if the objective lens is out of focus or the sample thickness slightly changes. The schematic diagram of the Z-contrast HADDF detector is shown in Figure 2.

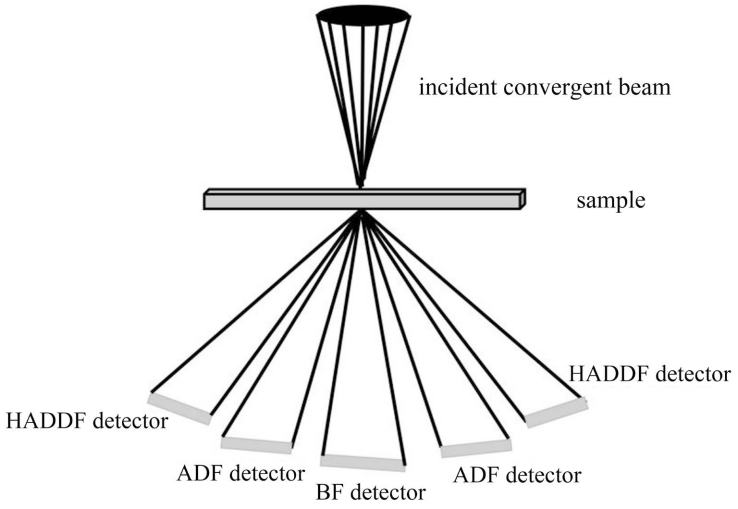

Figure 2. Schematic diagram of the Z-contrast image of the HADDF detector.

3. Experimental Research

3.1. Selection of Imaging Methods for Dispersion Analysis of Metal Particles

In recent years, with the development of the energy catalysis industry, transmission electron microscopy has attracted the attention of many researchers as one of the research tools for the microscopic morphology, elemental distribution, and crystal structure of nano and atomic scale materials. Among them, transmission electron microscopy, bright-field imaging, and dark-field imaging are key technologies in the catalyst research process, which can show morphological and structural details under specific thickness or diffraction contrast conditions. Bright-field image is used to characterize the catalyst morphology and support structure, collect low scattering angle electron signals to observe the overall morphology of the catalyst or support, through the bright-field image can observe the catalyst particle size, support pore structure and macroscopic arrangement, but usually the imaging contrast of metal nanoparticles with high Z contrast is low, the imaging is not ideal, and it is easy to be affected by electron beam damage. Dark-field images are preferentially selected for dispersion research. On this basis, high voltage will provide better penetration of the sample, the voltage is 200 KV, the high-angle annular darkfield image is about 100 pA probe current, the detector collection angle

range is 60 - 180 micro-radians, the camera length is 98 mm, and the electronic element distribution is realized in combination with EDS, and the characteristic X-ray photon characteristic energy is used to analyze the element types and distributions with different characteristics. In addition, it is worth noting that the selection of different test methods still needs to combine multiple factors, such as catalyst type, sample characteristics, and technical limitations.

3.2. Comparison of Different Carbon Film Supported Network Structures

The selection of carbon film carrier networks has a decisive impact on imaging quality, and the common types of carrier networks include ordinary unsupported carbon films, micro-gated porous carbon films, and ultra-thin carbon films [11], as shown in Figure 3. Ordinary unsupported carbon film is directly covered on the surface of the copper carrier network, which may lead to limitations in imaging electron beam-sensitive samples due to the uneven distribution of local thickness. The grid type is commonly used in microgrid porous carbon films, and the regular micropore size structure allows samples to be dispersed across pores, which can effectively prevent particles from accumulating on the surface of the continuous carbon film area. The ultra-thin carbon film has low background noise and can significantly improve the quality of high-resolution imaging, so the matching carbon film carrier network should be selected according to the sample characteristics to facilitate full observation. Taking the mesh film of the CSO instrument as an example, the comparison of key parameters of different carbon films used in TEM analysis is shown in Table 1.

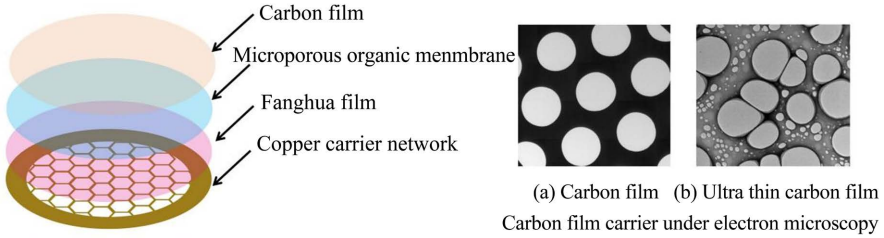

Figure 3. Comparison diagram of carbon film structure on the carrier network.

Table 1. Comparison of key parameters of different carbon films used in TEM analysis.

Carbon film carrier network	Approximate thickness/nm	Transparency	Application scenarios
Ordinary unsupported carbon film	10 - 20	High background noise and poor contrast	Routine topography observation
Microgrid porous carbon film	15 - 30 (No membrane in the hole)	No background noise, good contrast	High-resolution imaging
Ultra-thin carbon film	8 - 15	Low background noise and good contrast	Nanoparticles

3.3. Sample Preparation Method

Since nanoparticles have high surface energy and strong van der Waals interactions, small particles, in particular, will spontaneously agglomerate to reduce the free energy of the system. It is particularly important to choose an effective strategy to inhibit nanopowder aggregation. First of all, the compatibility with the sample and good dispersant volatility should be fully considered in the selection of the dispersant, and the dispersant should completely infiltrate the sample and not dissolve the carrier network to ensure that the sample can be dispersed at an appropriate speed and reduce the large-scale loss of local surface particles. Secondly, it is difficult to break the bond between the damaged particles by stirring or manual shaking, so it is necessary to use the ultrasonic method to treat the dispersion, and take the middle layer of liquid to eliminate the error caused by sedimentation or delamination, so as to ensure the data representativeness and dispersion reliability. The success of TEM sample preparation largely depends on the grasp of the above key steps, and the schematic diagram of the basic process of TEM powder sample preparation used in this paper is shown in Figure 4. The specific preparation steps are as follows.

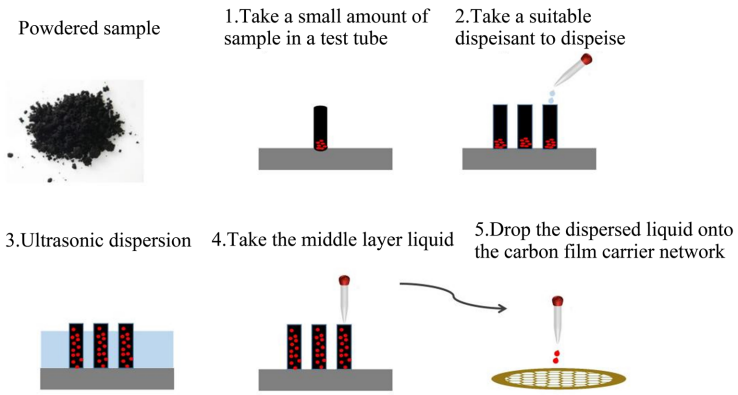

Figure 4. Preparation process of TEM powder samples.

3.4. Image Processing and Particle Size Statistics

The size distribution of nanoparticles for platinum/carbon catalysts was analyzed by TEM bright-field images, and the oxidation catalyst for diesel engine was analyzed in Velox software by HADDF-STEM images, and histograms of particle size distribution were plotted using Origin fitting or Excel software.

4. Results Analysis

4.1. Analysis of Imaging Contrast Effects

4.1.1. Analysis of the Effect of Carbon Film Carrier Network Characteristics on Background Contrast

The characteristics of the carbon film carrier network have a certain effect on the background contrast, as shown in Figure 5. Ordinary carbon film samples have a large thickness and poor light transmittance, and the carbon support is almost

integrated with the bottom of the back, and the carbon support profile cannot be recognized, resulting in unclear imaging, blurred catalyst particle boundaries, and inaccurate measurement of particle size. In order to enhance the clarity of the image and improve the contrast between the background and the sample to be tested, the ultra-thin carbon film carrier network is preferred.

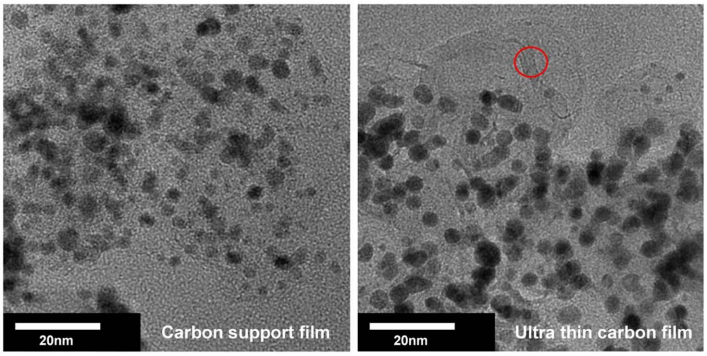

Figure 5. Imaging of different carbon film carrier networks.

4.1.2. Multi-Factor Synergy Analysis

Sample thickness, radiation damage, and defocus are the key variables regulating imaging contrast, and the key influencing factors of imaging contrast are shown in **Figure 6**. First, the thickness of the sample will directly affect the probability of electron penetration and scattering, and the contrast can be obtained by using the thickness difference of different micro-intervals of the sample, which is usually manifested in the brighter thin area and darker in the thick area. When the atomic number of the catalyst and the carrier is largely different, the signal intensity is correlated with the square of the atomic number, which inhibits the background noise caused by the carbon film [12], and the particle imaging is obvious. Therefore, HAADF-STEM mode imaging can be used when the difference in imaging contrast is not obvious in TEM mode.

Secondly, it is worth noting that radiation damage also has an impact on imaging contrast, which is mainly reflected in the electron beam irradiation time and the current of the electron beam spot. At the same time, the higher the current value, the greater the energy, and the local movement of the sample to be tested under the action of light and heat. For some amorphous carbon support films or loaded metal nanoparticles that are sensitive to electron beams, in order to avoid particle migration caused by carbon film shrinkage and rupture, it is necessary to optimize the voltage, beam balance resolution and damage, higher voltages can provide high resolution but will exacerbate knock-on damage, lower voltages will weaken the penetration of the electron beam, Therefore, the radiation damage mitigation should follow the principle of low dose, and only the beam spots converge in the target area during focus or image acquisition, and the shooting is completed in a short time. In terms of imaging contrast regulation, from another perspective, the regulation of defocus is particularly important; different contrast effects will occur under different conditions, and the particle boundary is clear in

the negative defocus state, which is convenient for particle size identification, and the lattice fringes are blurred. In the orthofocal state, the particle boundaries are not obvious, but the lattice stripes are clearer. The optimal amount of defocus often depends on the nature of the sample and observation requirements. Generally speaking, measuring the particle size is more suitable for underfocus, and looking at lattice fringes is more suitable for using positive focus.

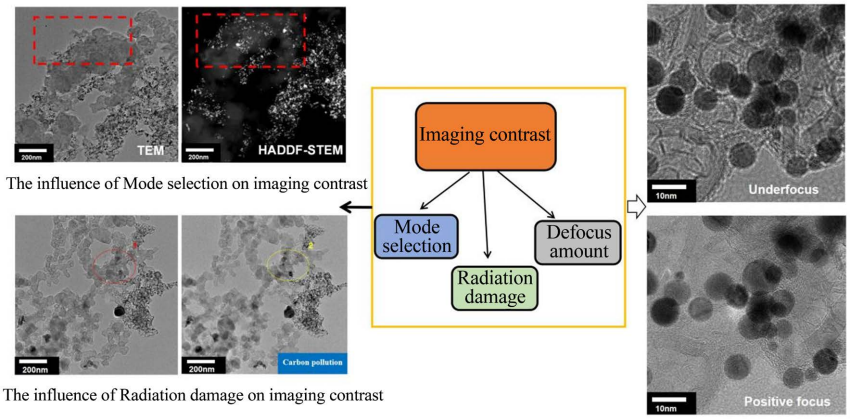

Figure 6. Key influencing factors of imaging contrast.

4.2. Physical Characteristics

The bright-field image is superimposed by diffraction contrast and thickness contrast, which is greatly affected by thickness factors, and the imaging depends on the local mass and thickness differences of the sample. The size change and distribution morphology of the platinum-carbon catalyst can be intuitively observed through TEM images, as shown in **Figure 7**. It is easy to observe that the graphitization characteristics of the support are highly anchored to small size, thin and dispersed Pt particles, and the Pt particles can be firmly anchored at the edge of the orderly exposure graphite, most of the particle size is distributed between 6 - 8 nm, the smallest size of the particles is about 2 nm, and the particle size is narrow.

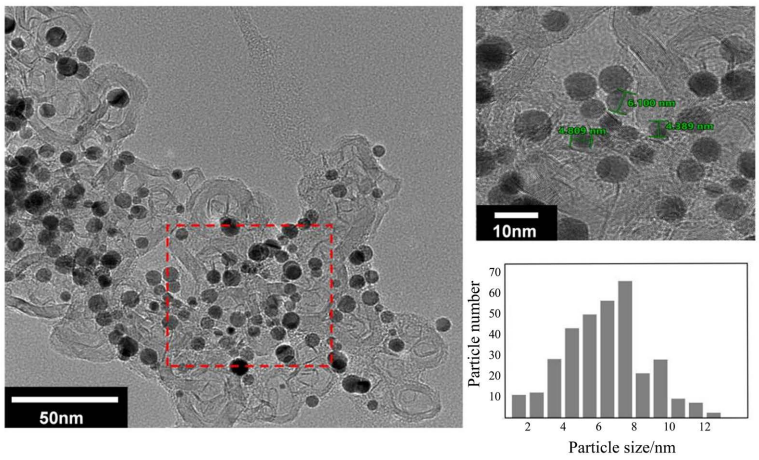

Figure 7. TEM diagram and particle size histogram of Pt/C catalyst.

Compared with bright-field imaging, factors such as thickness difference and atomic number similarity may lead to reduced contrast, resulting in misleading contrast and loss of morphological information of precious metal particles. This is because HADDF images in STEM mode are less affected by mass thickness contrast and phase contrast, are relatively insensitive to changes in sample thickness or density, and rely mainly on atomic number contrast imaging. The contrast diagram of TEM, HADDF-STEM and the elemental surface scan diagram of DOC catalyst are shown in **Figure 8**, from which it can be clearly seen that the contrast contrast under bright-field imaging is weak, making it difficult to distinguish particles, while the bright spots in **Figure 8** are Pt and Pd precious metal particles, which can clearly present the particle outline even in the thicker area of the sample. This is due to the difference in average intensity and standard deviation of images in the same area [13], and the extremely high contrast-to-noise ratio of HADDF-STEM images provides better distinction. The STEM-EDS elemental surface scan map shows the elemental distribution of the DOC catalyst, and the surface scan signal is evenly distributed on the surface of the support, with no obvious agglomeration observed.

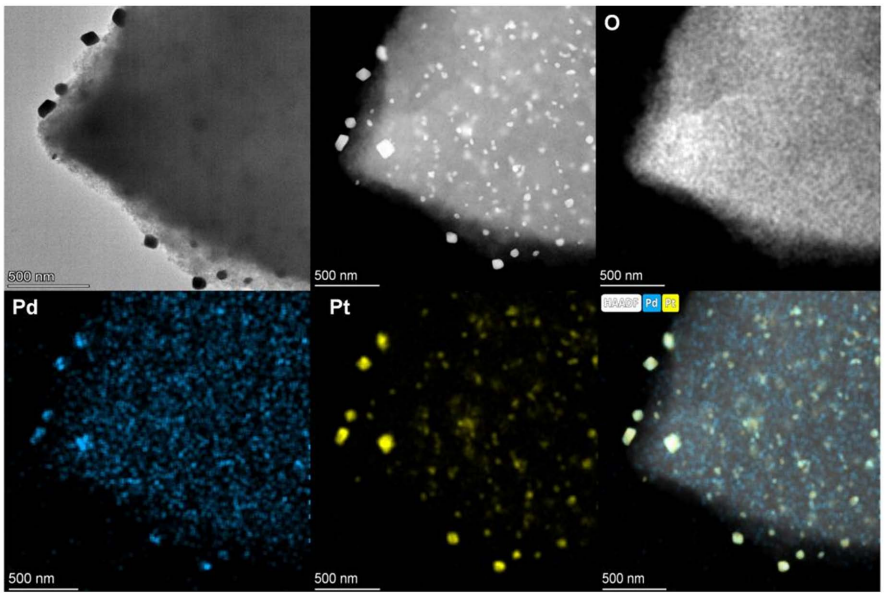

Figure 8. DOC catalyst TEM, HADDF-STEM, and EDS elemental surface scan diagram.

5. Conclusion

In this paper, the high-resolution imaging method of precious metal catalysts based on contrast differences is described by transmission electron microscopy, covering the imaging principle, sample preparation, method selection and testing links, focusing on the analysis of the correlation effect of imaging contrast under multi-factor conditions, taking platinum/carbon catalysts and diesel engine oxidation catalysts as examples to provide detection ideas and directions for different types of supported precious metal catalysts.

Conflicts of Interest

The authors declare no conflicts of interest regarding the publication of this paper.

References

[1] Larcher, D. and Tarascon, J. (2014) Towards Greener and More Sustainable Batteries for Electrical Energy Storage. *Nature Chemistry*, **7**, 19-29. https://doi.org/10.1038/nchem.2085

[2] Shih, C.F., Zhang, T., Li, J. and Bai, C. (2018) Powering the Future with Liquid Sunshine. *Joule*, **2**, 1925-1949. https://doi.org/10.1016/j.joule.2018.08.016

[3] Seh, Z.W., Kibsgaard, J., Dickens, C.F., Chorkendorff, I., Nørskov, J.K. and Jaramillo, T.F. (2017) Combining Theory and Experiment in Electrocatalysis: Insights into Materials Design. *Science*, **355**, eaad4998. https://doi.org/10.1126/science.aad4998

[4] Cheng, D., Hong, J., Lee, D., Lee, S. and Zheng, H. (2025) *In Situ* TEM Characterization of Battery Materials. *Chemical Reviews*, **125**, 1840-1896. https://doi.org/10.1021/acs.chemrev.4c00507

[5] Wang, G., Ke, X. and Sui, M. (2022) Advanced TEM Characterization for Single-Atom Catalysts: From *Ex-Situ* towards *In-Situ*. *Chemical Research in Chinese Universities*, **38**, 1172-1184. https://doi.org/10.1007/s40242-022-2245-0

[6] PONOR (2020) Teardrop-Shaped Electron-Matter Interaction Volume and Limits to the Depths from Which Each Signal Type Can Be Emitted or Detected. https://en.wikipedia.org/wiki/Scanning_electron_microscope

[7] Sanchez, S.I., Small, M.W., Sivaramakrishnan, S., Wen, J., Zuo, J. and Nuzzo, R.G. (2010) Visualizing Materials Chemistry at Atomic Resolution. *Analytical Chemistry*, **82**, 2599-2607. https://doi.org/10.1021/ac902089f

[8] Ford, B.J., Joy, D.C. and Bradbury, S. (2019) Transmission Electron Microscope. Encyclopædia Britannica, Inc. https://www.britannica.com/technology/transmission-electron-microscope

[9] Williams, D.B. and Carter, C.B. (2009) Transmission Electron Microscopy: A Textbook for Mate-Rials Science. 2nd Edition, Springer. https://doi.org/10.1007/978-0-387-76501-3

[10] Zhang, X.F. (2015) The History of Microscope and Microscopy. 2nd Edition, Tsinghua University Press. http://www.tup.tsinghua.edu.cn/booksCenter/book_06415001.html

[11] Goodhew, P.J. (1987) Specimen Preparation in Materials Science. Elsevier.

[12] Zaefferer, S. (2011) A Critical Review of Orientation Microscopy in SEM and TEM. *Crystal Research and Technology*, **46**, 607-628. https://doi.org/10.1002/crat.201100125

[13] Otsu, N. (1979) A Threshold Selection Method from Gray-Level Histograms. *IEEE Transactions on Systems, Man, and Cybernetics*, **9**, 62-66. https://doi.org/10.1109/tsmc.1979.4310076